Reticle programmed defect size measurement using low voltage SEM and pattern recognition techniques

Larry Zurbrick, KLA-Tencor Corporation, San Jose, CA, USA
Steve Khanna, KLA-Tencor Corporation, San Jose, CA, USA
Jay Lee, KLA-Tencor Corporation, San Jose, CA, USA
Jim Greed, VLSI Standards Incorporated, San Jose, CA, USA
Ellen Laird, VLSI Standards Incorporated, San Jose, CA, USA
Rene Blanquies, VLSI Standards Incorporated, San Jose, CA, USA

Abstract

The use of programmed defect test reticles to characterize automatic defect inspection equipment has long been an established practice in the maskmaking industry. Measurement of the defect sizes on these programmed defect test masks is not necessary if one only desires to qualitatively investigate differences in system performance. However, more meaningful comparisons in inspection system performance require a calibrated programmed defect test mask. Historically, commercially available programmed defect test reticles have not had traceable or well-documented defect sizing methods nor was information regarding the precision of these measurements provided. This paper describes the methods used and results obtained from the work performed to address these issues. Using a low voltage scanning electron microscope as an image acquisition system, defect sizing is accomplished using automated pattern recognition software. The software reports defect size metrics such as maximum inscribed circle diameter and area. Measurement precision better than 30 nm has been demonstrated for the maximum inscribed circle method. The correlation of SEM based measurements to historical optical metrology measurements is also discussed.

1 Introduction

Programmed defect test masks such as DuPont Photomasks' Verimask™ and Verithoro™ test masks are utilized to test defect detection sensitivity of automated defect inspection equipment. The defect size measurements provided with these test masks are stated as the one-dimensional height of the defect. These measurements are performed using a manually operated, visually based optical microscope utilizing an image shearing measurement method. This microscope uses white light supplied by a tungsten halogen lamp, a 100X 0.9 numerical aperture objective operating at a 0.7 sigma, and 10X eyepieces. For programmed defect sizes less than 0.5 μm and linewidths less than 1 μm, the repeatability of this measurement method is inadequate for ensuring inspection system performance specifications. **Figure 1** shows a histogram of the typical repeatability of this measurement method and the SEM measurement method discussed herein for a Verithoro™ 690EXS test mask. The histogram was constructed by performing a same defect pair-wise comparison between two sets of measurements, calculating the absolute difference between the defect measurement pairs, and binning these absolute differences.

Fig. 1 Comparison of Optical and SEM based measurement repeatability based upon paired measurement differences
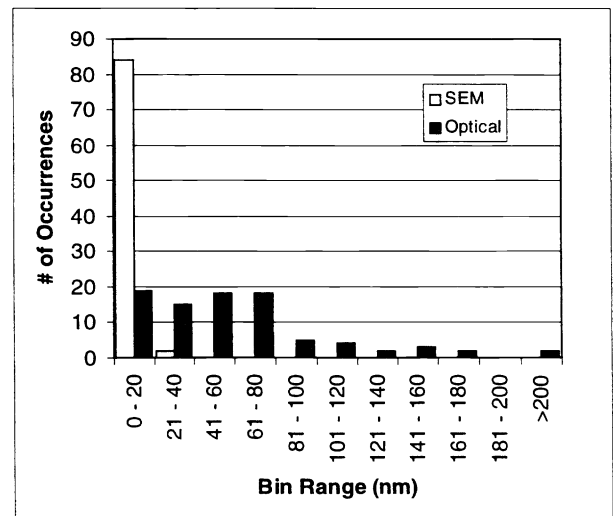
The optical measurement repeatability appears to be no better than 180 nm. The source of this lack of

repeatability is related to the small image scale (magnification) presented to the microscope operator and relatively large point spread function of the optics as compared to the defect sizes of interest (resolution). **Figure 2** illustrates the image scale that the microscope operator observes for a VT690EXS type test mask (the chrome edge defect is circled).

Fig. 2   Typical Optical measurement image scale
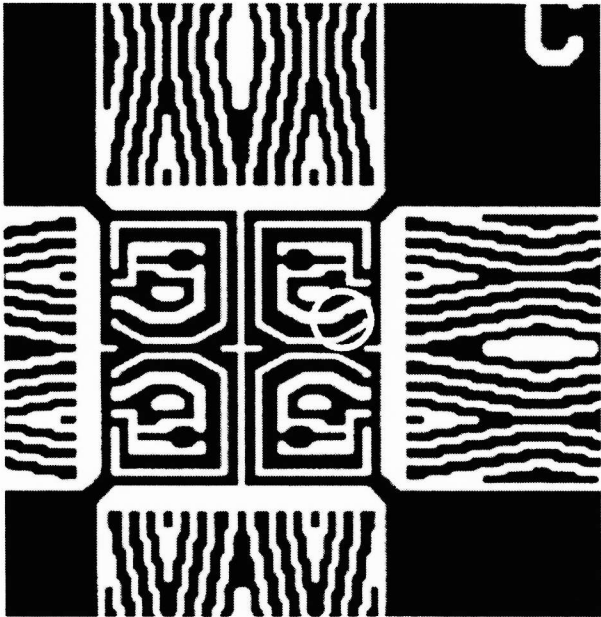
In order to improve the measurement repeatability, higher resolution and magnification are required. With the introduction of CD measurement scanning electron microscopes (SEM's) specifically designed for masks and reticles such as the KLA-Tencor 8100XP-R, issues of substrate handling and sample charging have been largely eliminated. **Figure 3** shows the same defect as Figure 2 imaged at 50KX with the KLA-Tencor 8100XP-R CD SEM. With the improve resolution, magnification and stored digital image, several different measurement methods (e.g. area, one dimensional height, XY bounding box) can be employed. However, a measurement method that closely correlated to historical optical measurements was desired.

Fig. 3   SEM image of defect shown in Fig. 2
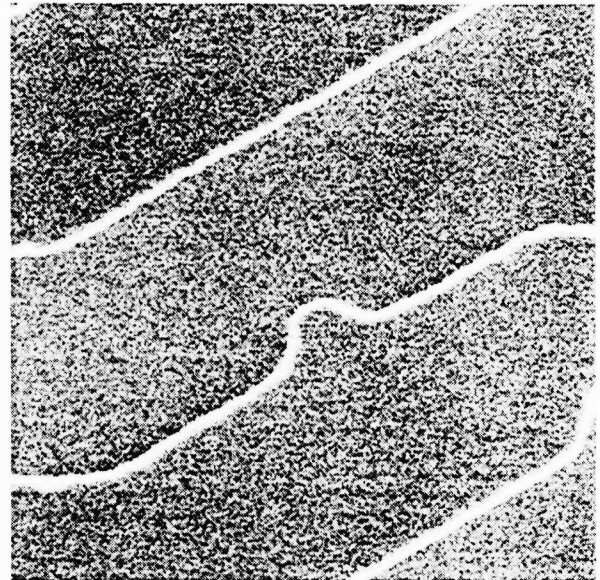
2   Experimental

Defect imaging was performed with a KLA-Tencor 8100XP-R CD SEM equipped with charge reduction hardware and utilizing secondary electron detection. The landing energies utilized for imaging were in the range of 1 to 2 kV.

Image analysis software was written to perform edge extraction, reference image alignment, defect extraction, and defect measurement on stored SEM digital images gathered with a KLA-Tencor 8100XP-R CD SEM. The image analysis operation utilizes a reference image (without a programmed defect) in order to perform the defect measurement. A reference image was utilized in order to compensate for intrinsic corner rounding on the test mask patterns. This was primarily done for the measurement of corner type defects. The defect measurements reported by the software include area, maximum inscribe circle diameter, and bounding box XY[1] dimensions.

To determine the correlation between historical optical measurements and SEM based measurements, SEM images from multiple Verithoro™ masks were gathered and defect size measurements and comparisons to the optical defect size measurements performed.

3 Results and Discussion

Initially, one dimensional defect height measurements were performed with the SEM mimicking the optical measurement method. It was soon discovered that programmed defect shape was not well controlled. **Figure 4** shows two chrome extension defects of approximately the same height from two different test masks. It can be seen that the defect shape varies considerably between the masks. It was decided that a SEM based one dimensional height measurement would not be adequate since it only provided limited information regarding the defect size. This also implied that a bounding box XY size measurement would have similar limitations (since the Y dimension of the bounding box is essentially the one dimensional defect height). Additionally, the X dimension of the bounding box could vary considerably depending upon line edge roughness and the gradual slope that exists at the base of some defects (referred to as "tails").

Fig. 4 Defects of similar height but different shape
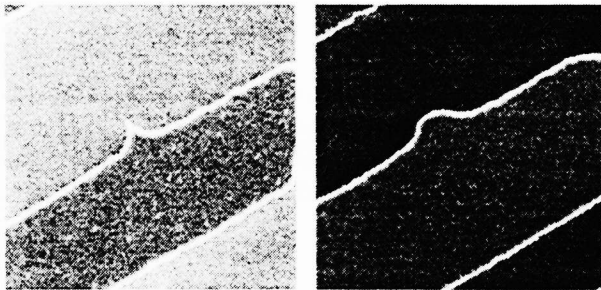
Defect square root of area was investigated as a defect size measure. The square root of area was of interest because it states defect size in terms of an equivalent "square defect" and that the measurement unit, micron (μm), is much more familiar than that of square microns (μm^2). It was observed that defect size based upon this measurement method could be influenced by sample line edge roughness and straightness on the defect and reference images. **Figure 5** illustrates this point. In figure 5, defect C3 (a chrome extension) from two different masks are compared. The reference edge is superimposed as a white line on the defect image along with the maximum inscribed circle. It can be seen that significant "tails" in terms of area can develop as in the case of the defect shown on the left (sn1019) of the figure as compared to the image on the right (sn1050). Although the defect on the left is smaller in height, it measures greater in square root of area. It was observed that the area in the "tails" can be greatly influenced by the edge roughness/straightness in the reference image. This type of change in defect area (i.e. low aspect ratio "tails) and its effect on defect printability is not entirely clear. Further investigations into the relationship of defect shape upon printability will be necessary. Additionally, use of square root of defect area for defects such as edge misplacements (CD error and misplaced contacts defects) and pinholes/pindots conflicts with the accepted definition for these defect types. It was desired to have a single measurement method that could be used for a wide range of defect types.

**Fig. 5** VT690EXS defect C3, sn1019 (left) and sn1050 (right)
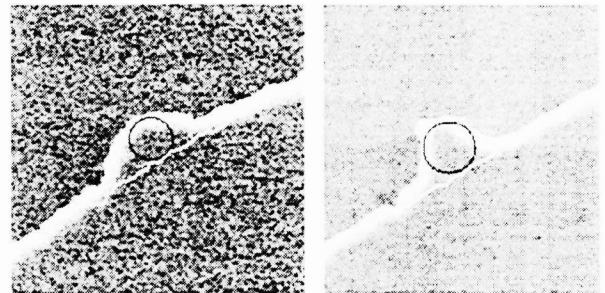
Sq. Root Area = 0.292 μm   0.266 μmMax.
Inscribed Circle = 0.18 μm   0.22 μm

A compromise between square root of area and one dimensional defect size is the maximum inscribed circle diameter method of measurement. This measurement method determines the maximum diameter circle that can be fit into the identified defect. This method has the advantage of working with edge misplacement, edge, corner, pinhole and pindot defects. See **Figure 6** for examples.
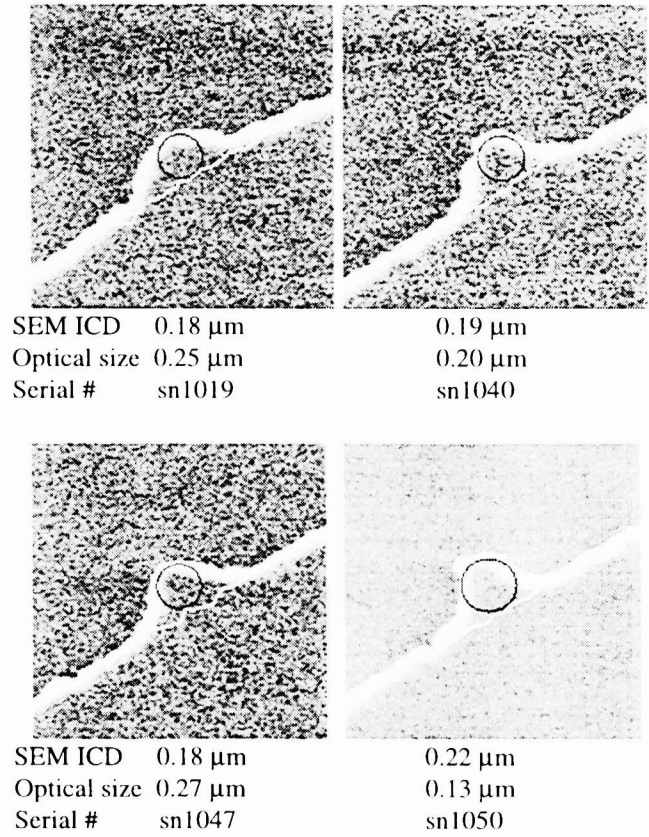
Fig. 6 Examples of maximum inscribed circle defect sizing method. Defect sizes range from 0.094 to 0.250 mm.
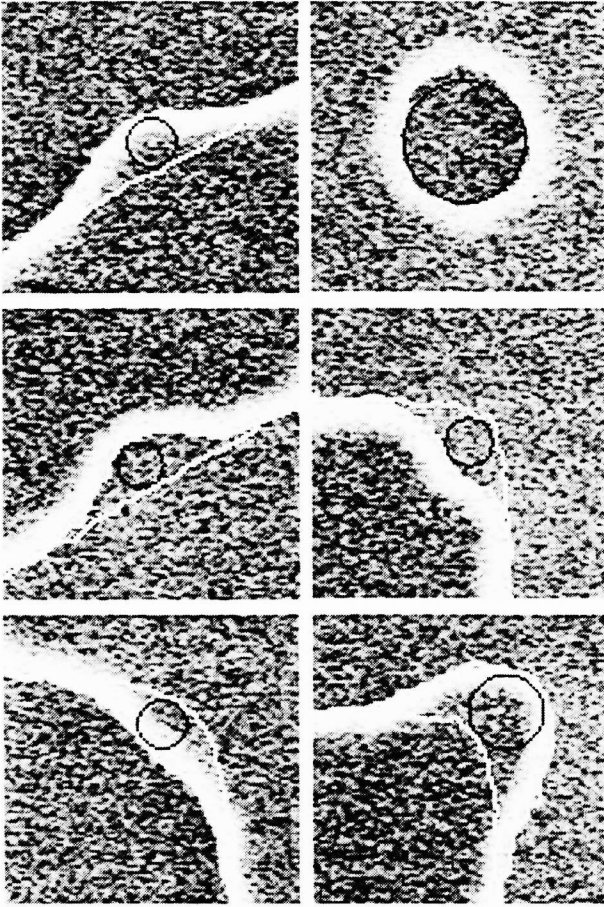
One of the largest issues in determining an average correlation between historical optical measurements and SEM based measurements was the variability in the historical optical measurements. Figure 1 shows the relationship between optical and SEM based Inscribed Circle Diameter (ICD) measurement repeatability for the same Verithoro™ 690EXS. The histogram was generated by performing a pair-wise comparison of measurements of the same defect on the same mask from two independent optical measurement data sets. As seen in Figure 1, 95% of the optical repeatability data extends over a range of 0 to 160 nm. Using the same test mask, three independent sets of SEM images were captured at 50KX magnification over the period of two weeks and the maximum ICD defect sizes determined using the image analysis software. The absolute size range was determined on a defect by defect basis and plotted on the same graph for comparison purposes. For the SEM based ICD measurement repeatability, 95% of the data is in the 0 to 20 nm range with a maximum observed difference of

30 nm. The defects included in this repeatability study include edge defects (rows A through D), corner defects (rows E through H), pinhole defects (row S), and pindot defects (row T). **Figure 7** shows defect C3 (chrome extension) from four different Verithoro™ 690EXS masks. All four defects appear to be similar in size and shape, with the SEM ICD sizes in the range of 0.18 to 0.22 μm. However, the optical one dimensional defect height measurements differ considerably ranging in size from 0.13 to 0.27 μm and do not appear to correlate to the SEM ICD sizes. The smallest optical measurement coincides with the largest ICD measurement (sn1050). Examination of the defect sizes and shapes reaffirms the belief that the optical measurement data is not repeatable.

Fig. 7 VT690EXS, defect C3, multiple test masks. Optical measurements show poor correlation to actual defect physical size

SEM ICD	0.18 μm	0.19 μm
Optical size	0.25 μm	0.20 μm
Serial #	sn1019	sn1040

SEM ICD	0.18 μm	0.22 μm
Optical size	0.27 μm	0.13 μm
Serial #	sn1047	sn1050

XY plots of the Optical minus SEM ICD measurement difference versus SEM ICD defect size were generated by defect type. See **Figures 8 and 9**. The different symbols in each plot represent a different serial number test mask. Analysis of this data showed that clear intrusions, clear notches on chrome corners, clear extended corners, and chrome notches on clear corners had an average

difference less than 0.05 μm over the defect size range studied with a slope close to zero. As these defect sizes approached 0.70 μm, the variability of the data decreased and approached a difference value within 0.05 μm of zero. It should be noted that the point spread function of the optical measurement instrument is approximately 0.75 μm in diameter. For extended chrome corners, values less than 0.60 μm averaged approximately 0.05 μm and did not appear to converge to zero for larger defect sizes. Chrome extension defects exhibited a more complex correlation behavior. Regression analysis of the chrome extension defects showed a positive slope of 0.267 μm/μm with an intercept of –0.019 over the defect size range studied. It is not entirely clear why chrome extension defects did not appear to converge to a fix value at the larger sizes, but may be due in part to the defects not reaching a large enough size. It also should be noted that the regression R^2 value was only 0.35 which indicates a very low degree of correlation. Pinhole defects exhibited two interesting behaviors. First, it appears that

the data is bimodal in that two distinct groupings of the data occur by serial number of test mask. The exact cause is not know, but may be related to an operator bias. This grouping of data does not occur for the other defect types. Second, the data appears to indicate that pinhole optical measurements change slope when the pinhole size is less than the optical measurement system's point spread function diameter, approximately 0.75 μm. Based upon apriori knowledge of the measurement characteristics of the optical tool, a 0.15 to 0.20 μm bias was expected between the two measurement techniques where the optical tool would measure pinhole sizes smaller (and the opposite being true for pindots). This is true for the upper group of the pinhole data larger than 0.75 μm. Pindot defect data exhibits a more random distribution with an average difference of 0.178 μm. The pindot defect optical measurements are larger than the SEM measurements which agrees with the apriori expectation.

Fig. 8 Defect size correlation for edge and corner defects

Defect Type A - Clear Intrusion

Defect Type B - Clear Intrusion

Defect Type C - Chrome Extension

Defect Type D - Chrome Extension

Defect Type E - Clear Notch on Chrome Corner

Defect Type F - Extended Chrome Corner

Defect Type G - Clear Extended Corner

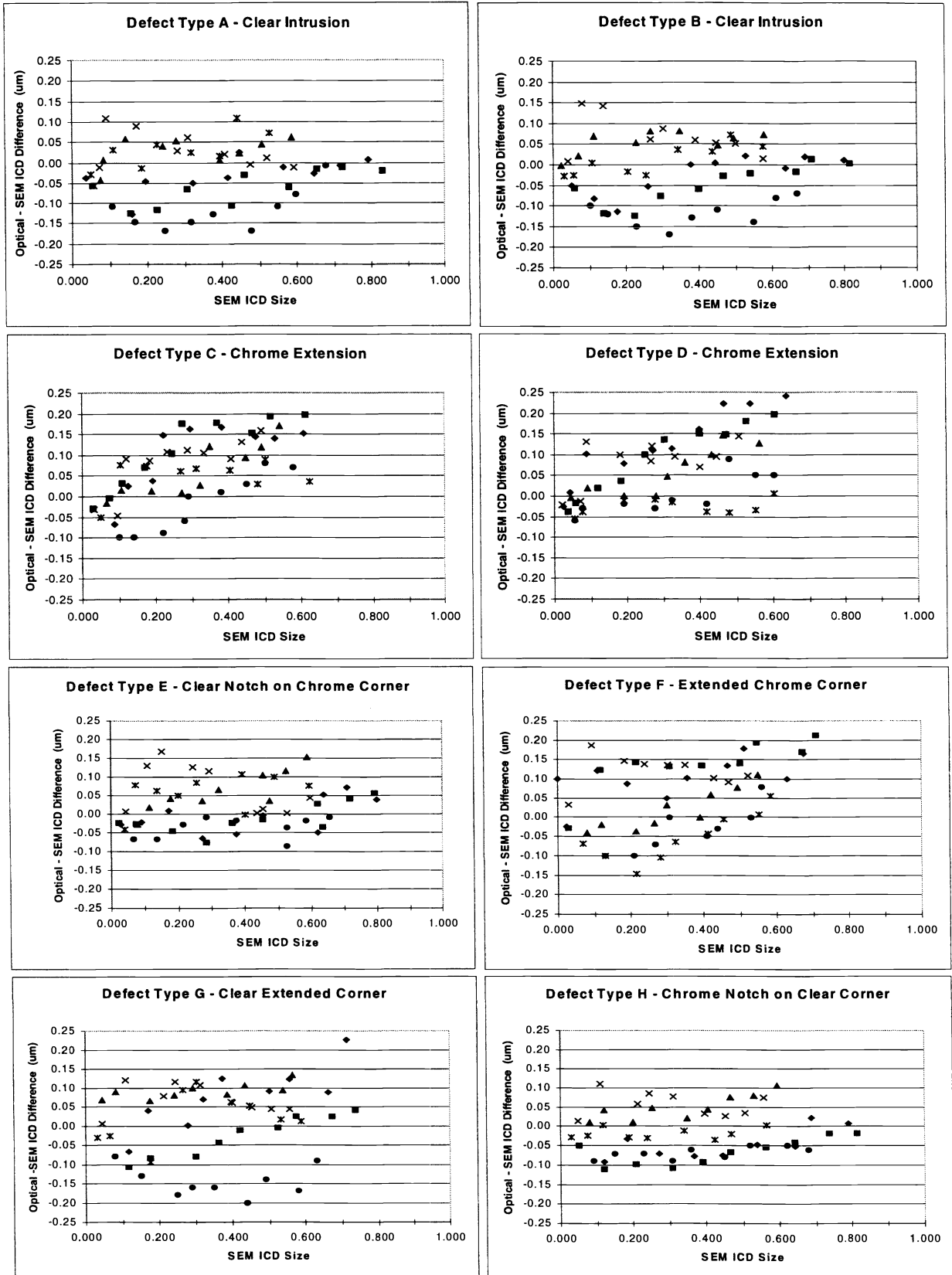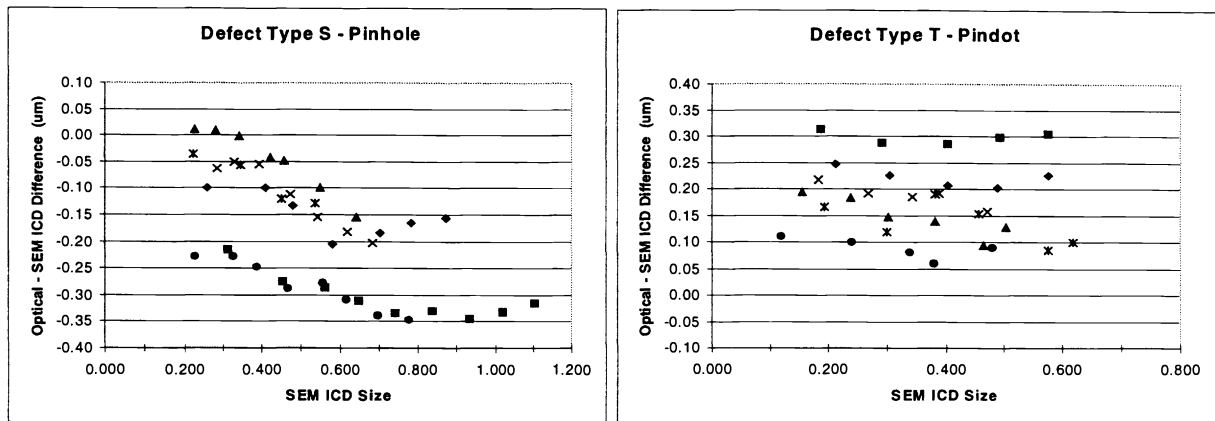Defect Type H - Chrome Notch on Clear Corner

Fig. 9 Defect size correlation for pinhole and pindot defects

4 Conclusions

Use of the KLA-Tencor 8100XP-R CD SEM and custom developed image processing software has improved defect sizing repeatability by a factor of 9X. The maximum inscribed circle diameter defect sizing method correlates with average historical optical measurements.

5 Acknowledgements

Verimask™ and Verithoro™ are trademarks of DuPont Photomasks Incorporated.

The authors would like to thank Lantian Wang of KLA-Tencor and Paul Konicek of VLSI Standards for performing SEM imaging work. The authors also thank DuPont Photomasks, Santa Clara, for use of their KLA-Tencor 8100XP-R CD SEM and providing optical measurement repeatability data.

6 Literature

[1] Semiconductor Equipment and Materials International (SEMI®) Draft Document 2780B, 13 October 1998, Revision to SEMI P22, Guideline for Photomask Defect Classification and Size Definition